

## Research Article

# Development of nanoemulsion loaded acyclovir nanogel for transdermal delivery and its evaluation

Tejas Suresh Telange, Shivani Santosh Pawar, Akash Jayendra Amkar, Bhushan Rajendra Rane\*, Ashish Suresh Jain

Shri D. D. Vispute College of Pharmacy and Research Center Panvel, Maharashtra, India

## ABSTRACT

Acyclovir (ACV) is an antiviral drug that is primarily used to treat herpes zoster virus (HSV) infections. HSV infections in deeper regions of the skin, i.e., nerve junctions, and appeared as a red spot on the upper part of the skin. The objective of the research is to formulate and evaluate an emulgel loaded with ACV microemulsion (ME) in order to treat herpes infections and to get effects from the deeper region of the skin. MEs were prepared by high-pressure homogenization, and then microemulgels were prepared by the dispersion method. Microemulgel characteristics are being determined, and an *in vitro* diffusion study was performed. In this study, we have developed and evaluated an ACV-loaded microemulgel using Carbopol 940 as the gelling agent. The characteristics and stability of ACV-loaded microemulgels were studied, and *in vitro* drug diffusion of the optimized microemulgel, i.e., MEG3, was found to be  $95\pm 2.4\%$  with a sustained effect for 8 hours. Observation shows that the optimized microemulgel has a smaller globule size, and hence it may move to the deeper regions of the skin. Stability studies did not show any significant change; hence, it is apparent that the drug substance or product will remain within the acceptance criteria during shelf life. It was concluded that the ACV-loaded microemulgel was prepared successfully for transdermal delivery.

### Keywords:

Microemulgel, Acyclovir, Transdermal, Surfactant, *In vitro* diffusion

## 1. INTRODUCTION

Acyclovir (ACV) is a class of antiviral medications called synthetic nucleoside analogues that mimic guanosine, which is defined by its structure (Figure 1). It is a first-line drug used to treat infections caused by HSV. ACV was approved by the Food and Drug Administration (FDA) to treat HSV encephalitis and genital herpes<sup>1</sup>. Some other non-FDA-approved indications are herpes zoster, varicella zoster, and mucocutaneous HSV, in which ACV can be used. It prevents the synthesis of viral agents by incorporating itself into the viral DNA<sup>2</sup>. The bioavailability of ACV is about 10-20%, which is considered to be much less, and the absorption through the topical route is not more than 10%. Therefore, in the current study, ACV is being used to get effective therapy, reduced side effects, and also reduced the dose of ACV through transdermal delivery<sup>3</sup>.

In the transdermal delivery system (TDDS), bioactive

ingredients are delivered across the skin to the systemic circulation. The application of drugs to the skin is considered to be one of the most important target sites<sup>4-6</sup>. It also provides controlled absorption, more uniform plasma levels, reduced side effects, painless and simple application, and the flexibility of terminating drug administration by simply withdrawing it from the skin<sup>7-8</sup>.

Microemulgels are dosage forms that have the properties of microemulsions as well as emulgels<sup>9-11</sup>. The prepared formulations are known as microemulgels when both microemulsion and gel are combined in the dosage form<sup>12-13</sup>. They offer a significant surface area for drug absorption, and the oil portion promotes bioavailability by enhancing drug permeability. Incorporating microemulsion into gel also increases its stability<sup>14-16</sup>. Microemulgel will be a more significant dosage form for the delivery of drugs through the transdermal route.

The current research is to prepare ACV-loaded microemulgels, which are considered to help reduce the side

### \*Corresponding author:

\*Bhushan R. Rane Email: rane7dec@gmail.com



Pharmaceutical Sciences Asia © 2023 by

Faculty of Pharmacy, Mahidol University, Thailand is licensed under CC BY-NC-ND 4.0. To view a copy of this license, visit <https://www.creativecommons.org/licenses/by-nc-nd/4.0/>

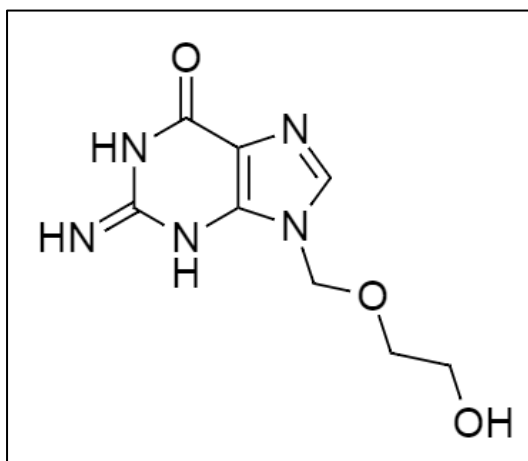


**Figure 1.** Structure of Acyclovir.

effects caused by the ACV. The formulated microemulgel is evaluated to determine its consistency, drug diffusion, viscosity, and stability to provide an effective therapy for HSV.

## 2. MATERIAL AND METHODS

### 2.1. Material

ACV was purchased from Mangalam Drugs & Organic Ltd., Mumbai; isopropyl myristate (IPM), Tween

80, polyethylene glycol 400 (PEG 400), ethanol, Carbopol 940, glycerine, methyl paraben, propyl paraben, triethanolamine, sodium chloride, potassium chloride, sodium phosphate dibasic, potassium phosphate monobasic, hydrochloric acid (HCl), and isopropyl alcohol were purchased from the Research-Lab Fine Chem Industries, Mumbai. The diffusion membrane was purchased from Dolphin Pharmacy Instruments Pvt. Ltd, Mumbai.

### 2.2. Spectroscopic studies

#### 2.2.1. UV spectrophotometric analysis for ACV determination

UV spectrophotometer (Shimadzu-1800, Shimadzu, Kyoto, Japan) was used for the estimation of the  $\lambda_{\max}$  of the ACV in phosphate buffer solution (pH 7.4) and methanol was determined, and the calibration curve was plotted by serial dilutions<sup>17</sup>. The  $\lambda_{\max}$  of ACV in a phosphate buffer solution (pH 7.4) and methanol was found to be 255 nm (Figure 2). The calibration curve in phosphate buffer solution (pH 7.4) shows a linearity range of 2-10  $\mu\text{g/mL}$ , the regression coefficient is 0.996, and the standard curve equation is found to be  $y=0.058x+0.006$ . In methanol, it shows a linearity range of 2-10  $\mu\text{g/mL}$ , while the regression coefficient is 0.995, and the standard curve equation is found to be  $y=0.046x+0.040$ .

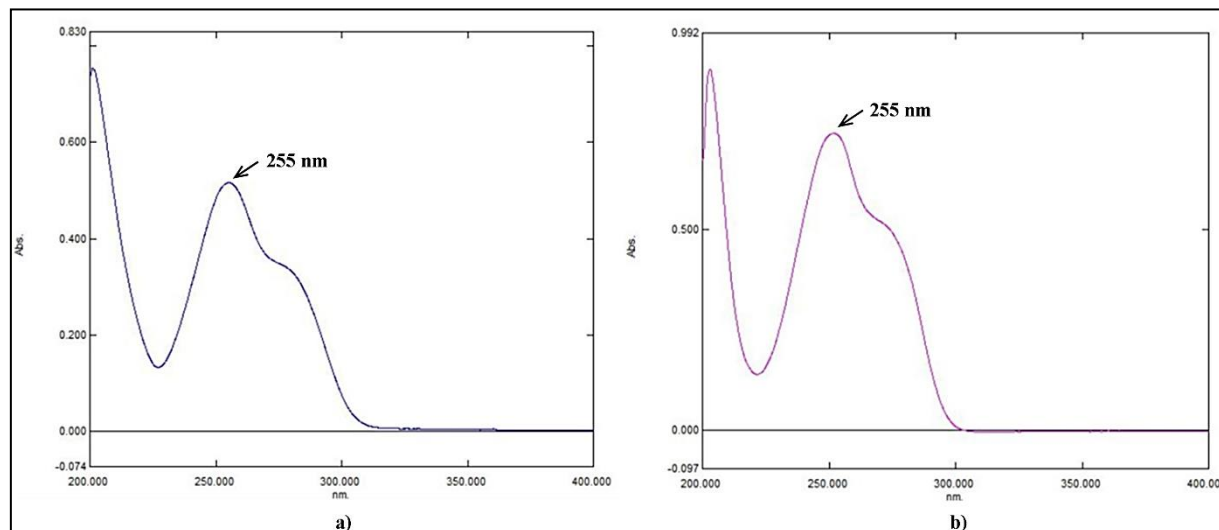


**Figure 2.** UV spectra in (a) methanol and (b) phosphate buffer solution (pH 7.4).

#### 2.2.2. FTIR Studies

IR analysis has been performed using Fourier-transform infrared (FTIR) spectrophotometer (IR Affinity-1, Shimadzu, Kyoto, Japan) on ACV, and the major components used in microemulgel preparation such as Tween 80, PEG 400, and Carbopol 940, all the spectra were compared with FTIR of the optimized microemulgel formulation. FTIR studies are performed for the determination of compatibility between ACV and excipients

by determining the standard peaks of drugs and other excipients in the FTIR of microemulgel. Previously dried solid samples of drug were placed in sufficient amounts on the crystal surface to fully cover it; the arm was twisted back to the center, and the knob was twisted clockwise until it was fixed at this position. For the FTIR of microemulgel, the semisolid sample of microemulgel was placed on the crystal, and the spectrum was recorded over a range of wavenumbers from 4,000  $\text{cm}^{-1}$  to 400  $\text{cm}^{-1}$ <sup>18</sup>.

### 2.3. Solubility studies for the screening of components

The solubility of ACV in different solvents and oils was determined using a UV-visible spectrophotometer (Shimadzu-1800, Shimadzu, Kyoto, Japan)<sup>18</sup>. The method used for the determination of solubility is the shaking flask method<sup>19</sup>. It was carried out by adding an excess amount of drug to each vial of a specific solvent and sealing it with a stopper. These vials were attached to an orbital shaker for 24 hours at a speed of 50 rpm, and a temperature of around  $37\pm 5^\circ\text{C}$  was maintained throughout the method. Each solution from the vials with suitable dilutions was prepared by using phosphate buffer solution (pH 7.4) and finally was scanned in a UV-visible spectrophotometer at 255 nm, and solubility was calculated. Oil, surfactant, and co-surfactant have been selected to formulate microemulsions of ACV based on the findings of solubility investigations<sup>20</sup>. The oils used in the research are olive oil, castor oil, and IPM, while the surfactant are Tween 20 and Tween 80, and co-surfactant is PEG 400<sup>21</sup>.

### 2.4. Construction of pseudo-ternary phase diagrams

The phase diagram was constructed using the method 'Aqueous Titration' to determine the region of microemulsion. So as to develop a microemulsion, different concentrations of water, selected oil, and surfactants and co-surfactants were blended<sup>22</sup>. Briefly, a mixture of oil, surfactant, and co-surfactant was prepared. The various weight ratios of surfactant to co-surfactant mixture (Smix) were taken as 1:1, 1:2, and 1:3. In a water titration, oil-phase solutions with surfactant and co-surfactant were produced in vials in the following ratios (% w/w): 1:9, 2:8, 3:7, 5:5, 6:4, 7:3, and 9:1<sup>23</sup>. A small amount of purified water, i.e., a 0.1 mL increment, was added to the vials. Following each addition, the mixture in vials was vortexed for 2-3 min and allowed to equilibrate for 5 min. After equilibration, the mixtures were examined visually for phase separation and transparency<sup>24</sup>. The point at which the mixture became turbid or showed signs of phase separation was considered the endpoint of the titration. This was allowed to stand overnight to observe any change in turbidity<sup>25</sup>. In order to reduce the turbidity of MEs, it was noted that the amount of purified water

needed as well as the proportions of the oil phase, Smix, and aqueous phase were plotted in a pseudo-ternary phase diagram using the CHEMIX School 10.00 programme (CHEMIX School 10.00, Arne Standnes, Bergen, Norway). The clear, stable, and emulsion zones were identified by using a ternary phase diagram<sup>26</sup>.

### 2.5. Preparation of ACV microemulsion

The pseudo-ternary phase diagram region for ME has been identified, and points from that region were chosen so as to cover the complete range of ME development in the phase diagrams with the lowest concentration of surfactant and the most amount of water<sup>27</sup>. In order to develop the microemulsions, 2% w/v of ACV was added to the oil phase and stirred on a magnetic stirrer for 20 to 30 min while being heated to  $30^\circ\text{C}$  to  $40^\circ\text{C}$  until the ACV solubilized in the oil. Additionally, a mixture of surfactant and co-surfactant (Smix) was prepared, and this Smix was added to the oil phase and thoroughly mixed again to get a homogeneous mixture of oil, surfactant, and co-surfactant (Table 1)<sup>28</sup>. Although the prepared emulsion is slightly clear, being an emulsion that contains globules larger than 500 nm, the prepared globule size might be non-homogenous in nature, which may not be suitable for transdermal delivery. So to get a reduction in globule size and a homogenous mixture of the globule size, it is treated with a high pressure homogenizer (HPH) (PandaPLUS 2000, GEA Niro Soavi, Italy) for the appropriate transdermal delivery. Hence, with the utilization of HPH, the globule size was further reduced to the nanosize of the formulated MEs. According to the reports, the pressure was tested on a placebo of microemulsion at 100, 200, 300, and 400 bars; since 400 bars lead to a smaller globule size, 400 bars was considered to be the ideal pressure for further experiments<sup>29</sup>.

### 2.6. Characterization of ACV microemulsion

#### 2.6.1. Drug entrapment efficiency

The centrifugation method was used to estimate the amount of ACV contained in ME. The supernatant was collected after 2 mL of ME had been centrifuged for

**Table 1.** Formulation table of nanoemulsion from pseudo ternary phase diagram.

Batch Code	IPM (mL)	Smix		Water (mL)
		Tween 80 (mL)	PEG 400 (mL)	
ME1	10	20	20	50
ME2	10	25	25	40
ME3	10	30	30	30
ME4	15	20	20	45
ME5	15	25	25	35
ME6	15	30	30	25
ME7	20	20	20	40
ME8	20	25	25	30
ME9	20	30	30	20

20 min at 5,000 rpm in a centrifuge tube, and a dilution was made in a 10 mL volumetric flask. Additionally, the volume was made up with methanol, scanned in a UV-visible spectrophotometer (Shimadzu-1800, Shimadzu, Kyoto, Japan) at 255 nm, and calculated<sup>30</sup>.

$$\frac{\text{Drug Entrapped}}{\text{Total Drug added}} \times 100 = \text{Entrapment Efficiency} \quad \text{Eq. (1)}$$

### 2.6.2. Thermodynamic stability of ME

The selected formulations were subjected to a thermodynamic stability study to assess their physical stability<sup>31</sup>. These studies were carried out with three different tests: the heating and cooling cycle test, the centrifugation test, and the freeze-thaw cycle test. During the heating and cooling cycles, the ME passed through six cycles between refrigerator temperatures of around 4°C and heating temperatures of around 40°C, with a storage period of 48 hours. In the centrifugation test, ME was subjected to centrifugation for 30 min at 5,000 rpm. In the freeze-thaw cycle, ME was kept in a deep freezer at -20°C for 24 hours, and after 24 hours, it was removed and kept at room temperature<sup>31</sup>. Further evaluation of ME is carried out on the specific ME that passed the thermodynamic stability test.

### 2.6.3. Globule size analysis and polydispersibility index (PDI)

The selected ME from the thermodynamic stability investigations is analysed for globule size and PDI to assess the globule size and homogeneity of the ME using the Malvern ZS instrument (Malvern ZS3000, Malvern Instrument Ltd, Worcestershire, United Kingdom)<sup>32</sup>.

**Table 2.** Formulation of an ACV-loaded microemulgel.

Sr. No	Ingredients	Formulation		
		MEG 1	MEG 2	MEG 3
1	Carbopol 940 (g)	1.00	1.50	2.00
2	Optimized ACV (400 mg) ME (mL)	42.11	42.11	42.11
3	Methyl Paraben (% w/w)	0.02	0.02	0.02
4	Propyl Paraben (% w/w)	0.01	0.01	0.01
5	Triethanolamine (mL)	1.00	1.00	1.00
6	Glycerin (mL)	2.00	2.00	2.00
7	Distilled Water (mL)	50.00	50.00	50.00

\*MEG: Microemulgel

## 2.8. Characterization of an ACV-loaded microemulgel

### 2.8.1. Appearance

The appearance of all the prepared microemulgels was checked visually for the presence of any aggregates or clumps. Microemulgels were evaluated by visualization to evaluate the presence of any visible particulate matter<sup>38</sup>.

### 2.6.4. Zeta potential

The ME's zeta potential was calculated using the Malvern ZS instrument (Malvern ZS3000, Malvern Instrument Ltd, Worcestershire, United Kingdom), which offers data on the stability of the ME and was selected based on thermodynamic stability tests of the optimized batch<sup>32</sup>.

### 2.6.5. Transmission electron microscopy (TEM)

Microscopy of the globules of the selected ME from the thermodynamic stability studies was carried out using TEM (Tecnai G2 spirit biotwin, FEI Company, Netherlands). ME was dropped on a carbon-coated grid that was positioned on a paraffin sheet, and the sample was kept on the carbon substrate to get the micro globules to adhere to it. Then phosphotungstate staining is applied to the grid for 20s. The prepared sample dried under the IR lamp, and then photographic images were captured by TEM<sup>33</sup>.

## 2.7. Preparation of microemulgel

Using a dispersion approach, an ACV-loaded microemulgel was developed by adding the ACV microemulsion to a hydrogel<sup>34</sup>. Carbopol 940 was used as a gelling agent in the preparation of the hydrogel. In order to make hydrogel, Carbopol 940 is appropriately weighed, dissolved in water while being stirred, and then the liquid is allowed to sit for 24 hours to allow for swelling<sup>35</sup>. For gel consistency, glycerin was added as necessary, and methyl and propyl parabens were added as preservatives<sup>36</sup>. Triethanolamine (1 mL) was added to the resulting microemulgel to neutralise it, and then the mixture was agitated to achieve transparency (Table 2)<sup>37</sup>.

### 2.8.2. Texture analysis

The TA.XT Plus instrument (TA.XTplus100C, Stable Micro System, Godalming, United Kingdom) is attached to the load cell. A 75-mm-diameter compression disc was used to compress a cylindrical shape of gel. TA.XT plus instrument was used to analyse the firmness and cohesiveness of the microemulgel in order to identify its textural characteristics.

**Firmness:** The maximum force achieved during the disc's downward movement denoted firmness.

**Cohesiveness:** Cohesiveness was defined as the amount of force required to raise the disc upward, which reflected a measure of the formulation's capacity to stick to the disc.

### 2.8.3. Determination of pH

The pH value of the prepared microemulgel was measured using a digital pH meter (EQ-610, Equiptronics, Sai Lab, India) that was calibrated before measurements<sup>39</sup>.

### 2.8.4. Determination of viscosity

The viscosity of the microemulgel with spindle number 93 of the T-series (Helipath) was measured using the Brookfield viscometer (DVT2 model, Brookfield Engineering Laboratories, Middleboro, USA). Viscosity measurements were carried out at 25°C, and the speed of the spindle was set to be 20 rpm.

### 2.8.5. Determination of spreadability

Using a modified wooden block and glass slide apparatus, spreadability was determined. It consists of a pulley at one end that provides a wooden block. A glass slide was fixed to the wooden block. 1 g of microemulgel was spread over the ground slide<sup>40</sup>. Microemulgel was squeezed between the ground slide and another glass slide, and then weight was applied to the slide to form a uniform film of the microemulgel between the slides<sup>41</sup>. Additional microemulgel was scraped from the edges. Using the string tied to the hook to support a weight of 20 g, the top slide was then moved down a distance of 7.4 cm, and the time it took to do so was recorded and calculated<sup>42</sup>.

### 2.8.6. Determination of extrudability

For determination of extrudability, a closed collapsible tube containing amicroemulgel of 20 g was pressed firmly at the curved end of the tube. The microemulgel was extruded from the tube as the cap was removed. The amount of the extruded microemulgel was collected and weighed, and then the percentage of the extruded microemulgel was calculated<sup>43</sup>.

### 2.8.7. % drug content

1 g of microemulgel was dissolved in a beaker containing Phosphate buffer solution (pH 7.4). The solution was sonicated for 3 cycles to ensure maximum drug dilution in the solvent. The sonicated solution was filtered, and 1 mL of filtrate was diluted into 20 mL of Phosphate buffer solution (pH 7.4). A UV-visible spectrophotometer

(Shimadzu-1800, Shimadzu, Kyoto, Japan) set to 255 nm was used to measure the drug content<sup>44-45</sup>.

### 2.8.8. In vitro drug diffusion study

A simple diffusion cell (Diffusion cell, Dolphin Pharmacy Instruments, Mumbai, India) was used to complete the *in vitro* drug release study. The cellophane membrane was mounted between the donor and the receptor compartments. The donor medium contained 1 g of ACV-loaded microemulgel, and the receptor compartment was filled with 40 mL of phosphate buffer solution (pH 7.4), while the temperature was set at 37±2°C. At different intervals, the aliquot samples were pulled out of the receptor compartment and replaced with fresh receptor medium in order to maintain the sink condition. Aliquot samples were filtered and then analysed for drug content by a UV-visible spectrophotometer (Shimadzu-1800, Shimadzu, Kyoto, Japan). The cumulative amount of drug release was determined as a function of time, and the release rate was calculated<sup>46-48</sup>.

The obtained release profiles were analyzed using model-dependent methods such as the Zero-order, First-order, Higuchi, Korsmeyer-Peppas, and Hixon-Crowell models.

The Zero-order kinetics model is as follows:

$$m_t = m_b + k_0 t \quad (\text{Eq. 2})$$

Where,  $m_t$  = Amount of drug release over time  $t$

$m_b$  = Amount of drug in solution before release

$k_0$  = Zero-order rate constant

The First-order kinetics model is as follows:

$$\ln(m_0 - m_t) = \ln(m_0) - k_1 t \quad (\text{Eq. 3})$$

Where,  $m_t$  = Amount of drug release over time  $t$

$m_0$  = Amount of drug in solution before dissolution

$k_1$  = First-order rate constant

The Higuchi model is as follows:

$$m_t = k_H t^{0.5} \quad (\text{Eq. 4})$$

Where,  $k_H$  = Higuchi rate constant

The Korsmeyer-Peppas model is as follows:

$$\log \frac{m_t}{m_\infty} = \log k_S + n \log t \quad (\text{Eq. 5})$$

Where,  $m_\infty$  = Amount of drug release after infinite time

$k_S$  = Korsmeyer-Peppas rate constant

$n$  = It is the parameter indicating drug release mechanism

The Hixon-Crowell model is as follows:

$$\sqrt[3]{m_0} - \sqrt[3]{m_i} = k_{HC}t \quad (\text{Eq. 6})$$

Where,  $m_i$  = Amount of drug left in the formulation over time  $t$

$k_{HC}$  = Hixon-Crowell rate constant

### 2.8.9. Stability study

The stability studies are carried out as per ICH guidelines Q1A (R2). Stability studies were performed according to ICH guidelines Q1A (R2) by keeping the optimized microemulgel at a temperature and relative humidity of around  $40 \pm 2^\circ\text{C}$  and  $75 \pm 5\% \text{RH}$  for a period of 3 months<sup>49-51</sup>. Samples from the microemulgel, which is kept for inspection, were withdrawn at definite time intervals<sup>52</sup>. The withdrawn samples were studied for changes in appearance, pH, spreadability, extrudability, drug content, and *in vitro* drug diffusion<sup>53</sup>.

## 3. RESULTS AND DISCUSSION

### 3.1. Selection and screening of ME components

#### 3.1.1. Screening of oil

Oil was screened based on its solubility, and it was also found to be non-toxic in nature for topical delivery. During studies, it was found that isopropyl myristate

(IPM) has the highest solubility, while olive oil and castor oil show less solubility as compared to IPM (Table 3). Thus, the study demonstrates that the IPM will be preferable for the preparation of ME.

#### 3.1.2. Screening of surfactant and co-surfactant

The surfactants selected should be less toxic in nature. Non-ionic surfactants are found to be less toxic in nature and also have low critical micelle concentration. Hydrophilic-lipophilic balance (HLB) is also an important factor in the consideration of surfactants. Some of the reports state that the required HLB value to form ME should be greater than 10<sup>54</sup>. The proper combination of surfactant and co-surfactant leads to the formation of stable ME. Therefore, the nonionic surfactant tween 80 was selected (HLB value 15) as compared to tween 20. Experimental results also state that the solubility of ACV in tween 80, i.e.,  $15.7 \pm 0.57 \text{ mg/mL}$ , is higher than in tween 20 ( $11.2 \pm 0.48 \text{ mg/mL}$ ) (Table 3). Nonionic surfactants were found to be less effective at lower pH of the formulation<sup>54</sup>. The miscibility of the proper amount of surfactant and oil gives clear MEs. A low volume of surfactant and co-surfactant is used to get stable ME. PEG 400 was selected as a co-surfactant because it has a high solubilizing capacity of ACV, i.e.,  $18.3 \pm 0.79 \text{ mg/mL}$  (Table 3), and it also has good permeation ability, which helps in permeation during topical delivery<sup>55</sup>.

**Table 3.** Solubility of ACV in different solvents, surfactants, and co-surfactants.

Sr. No.	Solvent	Solubility (mg/mL)
1.	Olive oil	$2.1 \pm 0.12$
2.	Castor oil	$2.3 \pm 0.19$
3.	IPM	$2.8 \pm 0.23$
4.	Tween 20	$11.2 \pm 0.48$
5.	Tween 80	$15.7 \pm 0.57$
6.	PEG 400	$18.3 \pm 0.79$

\*Note: All the studies were carried out in triplicate

### 3.2. FTIR analysis

FTIR studies are carried out to study the compatibility between the major components used in microemulgel preparation, which are Tween 80, PEG 400, and Carbopol 940, as compared with ACV.

In the Figure 3, FTIR of the drug shows the characteristic peaks at  $3,306 \text{ cm}^{-1}$  that attribute to O-H stretching; C-O stretching was observed at  $1,719 \text{ cm}^{-1}$ , at  $3,523 \text{ cm}^{-1}$   $\text{NH}_2$  stretching was observed; and C-N stretching was observed at  $1,632 \text{ cm}^{-1}$ . These characteristic peaks observed indicate the conformation and purity of the drug.

In the Figure 3, FTIR of the optimized formulation studied for compatibility studies shows the peaks at  $3,308 \text{ cm}^{-1}$  attribute to the O-H stretching, the peak observed at  $1,711 \text{ cm}^{-1}$  shows the C-O stretching,  $\text{NH}_2$  stretching was observed at  $3,517 \text{ cm}^{-1}$ , and the peak observed at  $1,634 \text{ cm}^{-1}$  shows the characteristic peak of C-N stretch-

ing. These observed peaks in the optimized formulation are found to be matched with the peaks observed in the FTIR of the drug. Other peaks observed are  $1,735 \text{ cm}^{-1}$ , which might resemble the C=O stretching of tween 80; a peak at  $1,249 \text{ cm}^{-1}$  may attribute to the C-O-C stretching of PEG 400; a peak observed at  $1,296 \text{ cm}^{-1}$  may attribute to the C=O stretching of PEG 400; and a peak at  $802 \text{ cm}^{-1}$  may resemble the C=C stretching of Carbopol 940.

These FTIR studies estimate that there were no interactions between the ACV and excipients. Hence, it states that the drug and excipients are compatible with each other within the formulation (Figure 3).

### 3.3. Construction of a Pseudo-Ternary Phase Diagram

The screening of ME components for oil selection, surfactant, and co-surfactant was previously discussed.

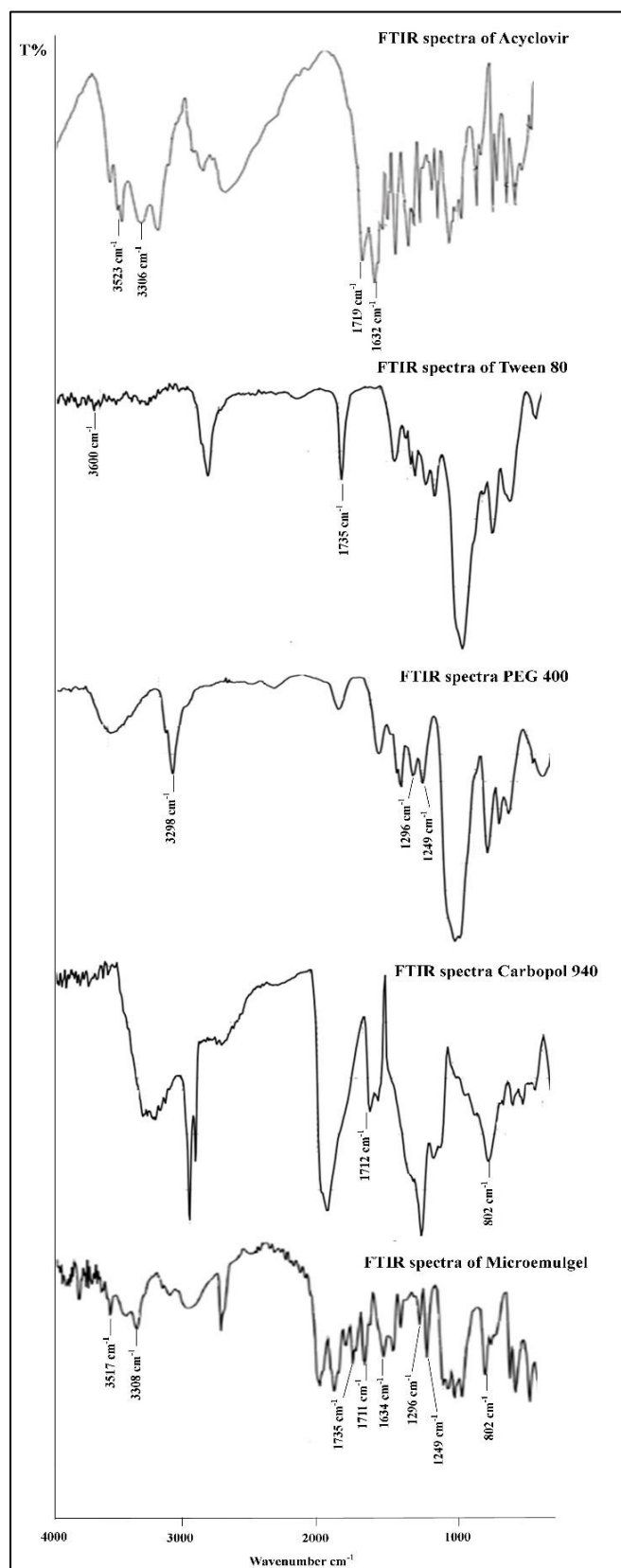


**Figure 3.** FTIR spectrum of the ACV, Tween 80, PEG 400, Carbopol 940, and Microemulgel.

Additionally, the selection of the amount of oil, surfactant, and co-surfactant was analysed and determined by using a pseudo-ternary phase diagram to get a proper, stable,

and clear ME and to minimize the runs for the preparation of ME. A pseudo-ternary diagram is plotted using CHEMIX School 10.00 programme (CHEMIX School 10.00, Arne Standnes, Bergen, Norway). Observations from the prepared phase diagram demonstrate that the region found in the diagram is suitable for the preparation of ME, while the ratio is found to be 1:1 for tween 80 and PEG 400 because it shows the broadest area in the diagram and might show maximum solubilizing capacity as per solubility studies (Figure 4).

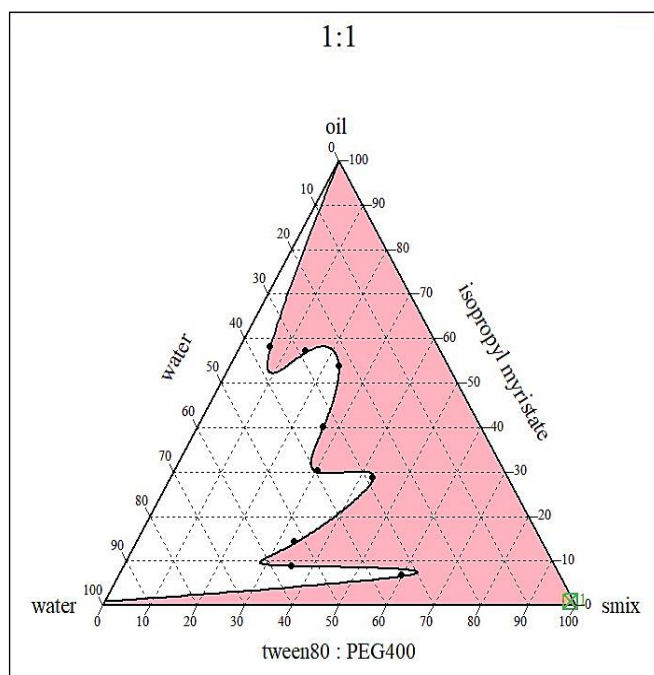


**Figure 4.** Pseudo-Ternary Phase Diagram for IPM, Smix, and Water.

### 3.4. Characterization of ACV Microemulsion

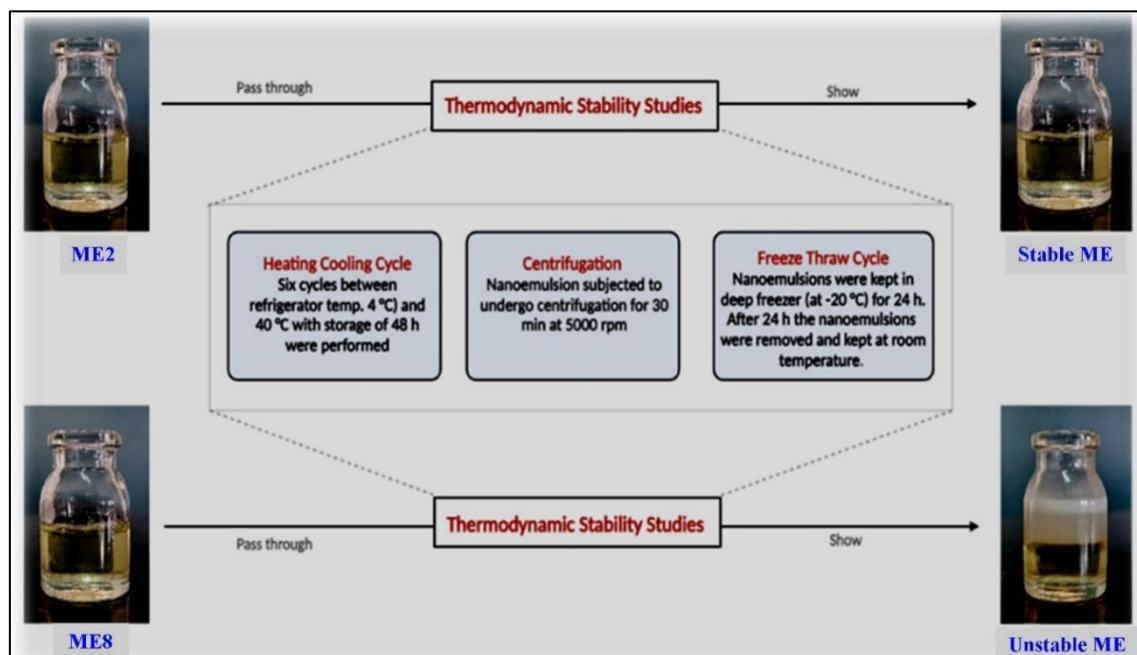
#### 3.4.1. Entrapment efficiency and physical appearance of ME after 24 hours

According to the pseudo-ternary phase diagram, the batch was prepared, and the entrapment efficiency of formulated batches shows that the percentage of entrapment is about 78.64% to 91.20%. The highest entrapment was shown by batches ME2 and ME8 because ME2 and ME8 consist of a Smix concentration of about 50% of the formulation, which makes stable and intact globules and thus will not diffuse the drug into water during the preparation method of microemulsions<sup>60</sup>. Hence, this might be the reason for the highest entrapment in ME2 and ME8 as compared to the other MEs. Formulations ME2 and ME8 also show a clear appearance after 24 hours of preparation, while other batches do not show transparency for selection for further studies (Table 4). Some of the MEs were found to have phase separation after being kept for several days and hence ME2 and ME8 were selected for further studies.

**Table 4.** %EE and observation after 24 hours of prepared MEs.

Batch code	Observation after 24 hours	Entrapment Efficiency (%)
ME1	Hazy	87.26 ± 1.7
ME2	Clear	91.20 ± 1.9
ME3	Almost Clear	81.02 ± 1.6
ME4	Hazy	84.24 ± 1.8
ME5	Almost clear	78.64 ± 2.1
ME6	Hazy	86.38 ± 1.8
ME7	Almost clear	81.42 ± 1.9
ME8	Clear	90.40 ± 2.4
ME9	Hazy	85.30 ± 2.2

\*Note: All the studies were carried out in triplicate

**Figure 5.** Thermodynamic stability study of ME2 and ME8.

### 3.4.2. Thermodynamic stability of MEs

From the above test, it was found that ME2 and ME8 were stable batches as per appearance and showed no separation of phases during storage. Therefore, ME2 and ME8 were subjected to thermodynamic stability studies. The thermodynamic stability of batches ME2 and ME8 was tested to ensure their stability at various temperatures. ME2 was found to be a more stable batch as it passed all the conditions of heating and cooling cycles, centrifugation, and freeze-thaw cycles and showed no phase separation, while ME8 passed the conditions of heating and cooling cycles and centrifugation but showed phase separation in freeze-thaw conditions (Figure 5). According to this observation, batch ME2 was more stable than batch ME8.

As a result of the thermodynamic stability test, the ME2 formulation is considered to be more physically stable.

### 3.4.3. Globule size and PDI

The PDI of the ME2 was found to be 0.262, indicating

a narrow size distribution. The average globule size of the ME2 was discovered to be  $227.4 \pm 16.24$  nm, demonstrating that the globules are less than 250 nm in size (Figure 6a). In addition, reports claim that the oil concentration affects the globule size; the greater the oil concentration, the larger the globule size<sup>61</sup>. Our work also shows that modest amounts of oil produce globule sizes less than 250 nm<sup>62</sup>. This indicates that the desired globule size was achieved, and it helps to permeate the drug through the skin<sup>61-62</sup>.

### 3.4.4. Zeta Potential

The Zeta potential study found that the ME is negatively charged. The zeta potential result of ME2 showed a value of  $-31.2 \pm 4.12$  mV (Figure 6b). Reports indicate that the value above or below  $\pm 30$  mV indicates a highly stable formulation<sup>63</sup>.

### 3.4.5. TEM

A TEM study of ME2 was conducted, and the results show that the morphology of the globules was spherical

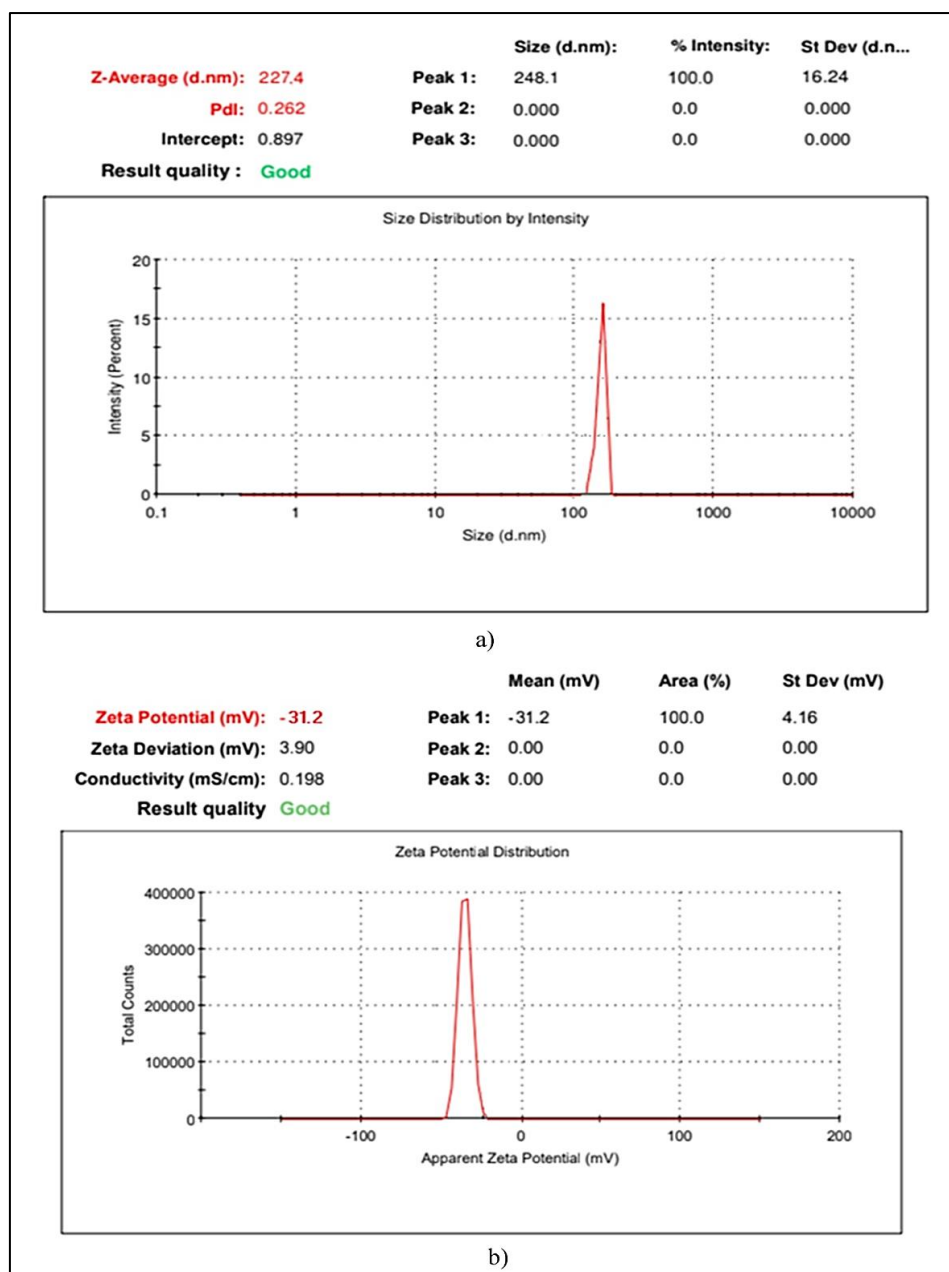


Figure 6. a) Globule size and b) Zeta potential of ME2.

in shape. Additionally, a significant number of globules were discovered to be less than 260 nm, which has already been covered in the globule size analysis. The TEM study confirms that the prepared ME has the desired globule size, and no agglomeration of globules is found between them, which states that ME is in stable form (Figure 7).

So, from the above results for ME2, it is found that ME2 has suitable characteristics for the delivery of ACV through the transdermal route. Hence, ME2 is considered ideal for the preparation of microemulgels.

### 3.5. Evaluation of ACV-loaded Microemulgel

#### 3.5.1. Appearance

All the prepared formulations of microemulgels

showed a good appearance and were free from any particulate matter (Table 5).

#### 3.5.2. Texture analysis

Texture analysis was performed to evaluate the firmness and cohesiveness of the microemulgels. The firmness of MEG3 was found to be  $60.12 \pm 0.49$  g, while for MEG2 and MEG1, it was found to be  $58.28 \pm 0.78$  g and  $57.48 \pm 0.76$  g, respectively. The MEG3 shows high consistency, and the cohesiveness obtained is  $-38.47 \pm 0.71$  g as compared to the MEG2 and MEG1, which show less cohesiveness, i.e.,  $-49.11 \pm 0.47$  g and  $-56.34 \pm 0.42$  g, respectively. Results suggest that the firmness and cohesive nature of MEG3 are high. Thus, the above outcomes suggest that microemulgel will be capable of having

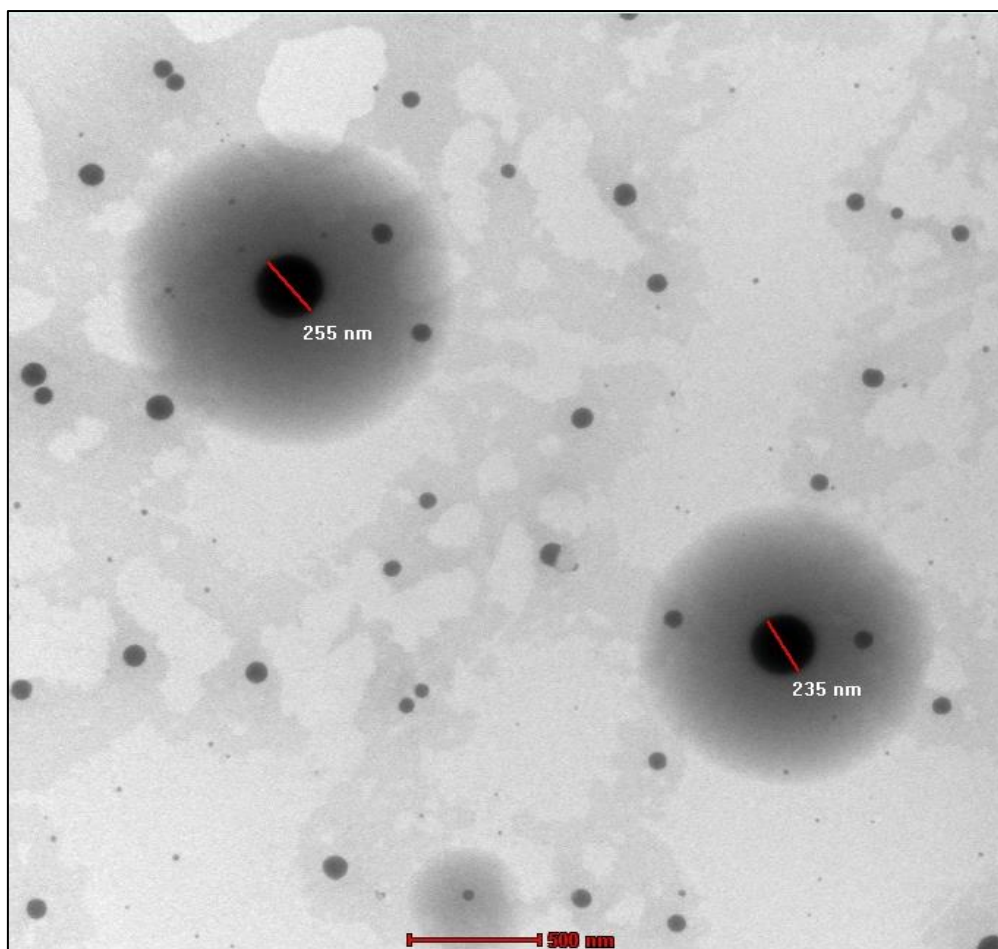


**Figure 7.** TEM microscopic photography of ME2.

**Table 5.** Formulations of microemulgels and their evaluated parameters.

Formulation	Appearance	Firmness (g)	Cohesiveness (g)	pH	Viscosity (cps)	Spreadability (g.cm/s)	Extrudability (%)	Drug content (%)
MEG1	++	57.48 ± 0.76	-56.34 ± 0.42	6.93	46248 ± 37.21	5.92 ± 0.28	80.87 ± 1.25	97.45 ± 1.14
MEG2	+++	58.28 ± 0.78	-49.11 ± 0.47	6.98	46457 ± 69.17	3.52 ± 0.18	83.14 ± 1.91	98.14 ± 1.34
MEG3	+++	60.12 ± 0.49	-38.47 ± 0.71	7.05	46669 ± 48.31	2.74 ± 0.08	85.37 ± 1.64	98.79 ± 1.08

\*Note: All the studies were carried out in triplicate.

MEG: Microemulgel

+: Turbid

++: Clear

+++ : Very Clear

appropriate spreadability on the skin and ease of application, while it might not cause difficulty during extrusion from the container<sup>58</sup>.

### 3.5.3. pH

The pH of all the formulated microemulgels was found to be in the range of 6.93 to 7.05. The normal and acceptable range of the skin is 6 to 7.4<sup>64</sup>. Hence, all microemulgels have an acceptable pH range (Table 5).

### 3.5.4. Viscosity

The measurements of the viscosity of the prepared microemulgels were carried out. MEG3 shows a high

viscosity of about 46,669±48.31 cps as compared to MEG1, and MEG2 shows 46,248±37.21 cps and 46,457±69.17 cps, respectively (Table 5). Thus, the study demonstrates that the viscosity increases with an increase in the concentration of Carbopol 940.

### 3.5.5. Spreadability

Based on calculations, it has been discovered that the spreadability of designed gel microemulgels lies between 2.74 and 5.92 g.cm/s (Table 5). These results clearly state that the MEG3 has a minimum spreadability effect while covering a smaller area and might show a targeted effect as compared to the MEG1 and MEG2.

### 3.5.6. Extrudability

The extrudability of MEG3 shows maximum extrudation, i.e.,  $85.37 \pm 1.64\%$  of microemulgel from the collapsible tube, when the force is applied, while MEG1 and MEG2 have less extrudation, about  $80.87 \pm 1.25\%$  and  $83.14 \pm 1.91\%$ , respectively (Table 5).

### 3.5.7. % drug content

The drug content of the microemulgel does not vary much, ranging from 97.45% to 98.79% (Table 5). MEG3 shows a high percentage of drug content in comparison with MEG1 and MEG2.

### 3.5.8. In vitro diffusion study

Membrane diffusion was used to determine the *in vitro* release studies of the microemulgel formulation

using a simple diffusion cell. Phosphate buffer solution (pH 7.4) (solubility: 2.21 mg/mL) was used for the receptor compartment during the release tests, and microemulgel was used for the donor compartment throughout the duration of the experiment, up to the point at which ACV was released to its maximum level. Results state that the percentage of drug released is found to be in the order MEG3>MEG2>MEG1, while the sustaining period is also found to be in the same order. The MEG3 had the longest sustaining time, which was 8 hours with a  $95 \pm 2.4\%$  released ( $p < 0.05$ ), while the MEG2 and MEG1 had durations of sustained release of ACV of 7 hours with an  $81 \pm 2.3\%$  released and 6 hours with a  $75 \pm 2.8\%$  released, respectively (Figure 8). In MEG3, the concentration of Carbopol is high as compared to MEG2 and MEG1, which might affect the sustaining effect of ACV release. An increase in Carbopol concentration forms a compact matrix-like structure, which will release the ACV at a slow pace and provide sustained release<sup>65</sup>.

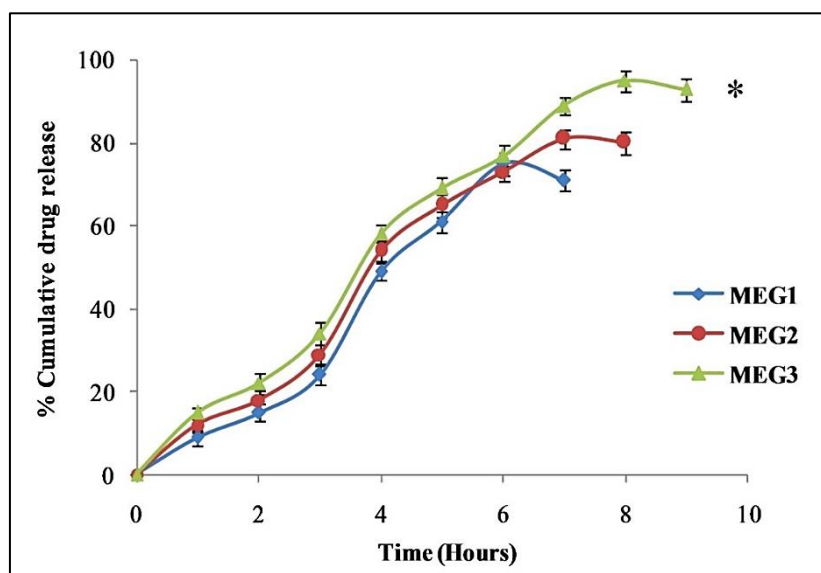


**Figure 8.** *In vitro* drug release of ACV from microemulgel in phosphate buffer solution (pH 7.4) (n=3, mean±S.D., \* $p < 0.05$ ).

### Drug release kinetics study

DD solver software was used to apply kinetic models to determine the ACV release from the microemulgel.

From the above findings the best fit model for the prepared formulation is Korsmeyer-Peppas model as the  $R^2$  values is close to the 1. As the Korsmeyer-Peppas models is much more suitable for the unknown drug release mechanism from the polymeric matrix. The model suggest that the drug release involves two mechanisms are polymer relaxation and diffusion. The  $n$  value of the MEG proposed that the drug release is non-Fickian because  $n < 1$  in which release is governed by diffusion and swelling from the MEG (Table 6)<sup>62</sup>. Also release rate constant does not showing any significant differences within the MEG thus it considers that the prepared formulation is following the Korsmeyer-Peppas model.

From the above results of prepared microemulgels, MEG3 was found to be the best preparation, as it shows better results compared with other microemulgels. Hence, MEG3 is considered an optimized microemulgel and further loaded for the stability study.

### 3.5.9. Stability Study

The stability studies of the ACV-loaded microemulgel were estimated for the optimized formulation, MEG3. From the study, it was observed that there was no change in appearance, texture characteristics, pH, viscosity, spreadability, extrudability, or drug content (Table 7). As observed, the accelerated data for any attribute did not show any significant change over time, making it apparent that the drug substance or product will remain within the acceptance criteria.

**Table 6.** Release rate constants and R<sup>2</sup> values of the formulated microemulgel.

Formulation Code	Zero order		First order		Higuchi		Korsmeyer-Peppas			Hixon crowell	
	R <sup>2</sup>	k <sub>0</sub> (%/h)	R <sup>2</sup>	k <sub>1</sub> (h <sup>-1</sup> )	R <sup>2</sup>	k <sub>H</sub> (%/h <sup>1/2</sup> )	R <sup>2</sup>	k <sub>s</sub> (h <sup>-n</sup> )	n	R <sup>2</sup>	k <sub>Hc</sub> (% <sup>1/3</sup> /h)
MEG1	0.957	12.00	0.934	0.22	0.858	29.93	0.960	16.47	0.83	0.956	0.06
MEG2	0.949	11.13	0.899	0.16	0.793	24.20	0.953	12.27	0.76	0.922	0.04
MEG3	0.957	12.11	0.933	0.22	0.892	30.01	0.971	19.38	0.85	0.964	0.07

**Table 7.** Stability study data of MEG3.

Formulation Code	MEG3			
Storage Condition	40 ± 2°C; 75 ± 5 %RH			
Time Interval (Days)	0	30	60	90
Appearance	+++	+++	+++	++
Firmness (g)	60.12 ± 0.49	60.05 ± 0.41	59.83 ± 0.37	59.80 ± 0.31
Cohesiveness (g)	-38.47 ± 0.71	-38.31 ± 0.42	-37.97 ± 0.56	-37.69 ± 0.49
pH	7.05	7.00	7.00	6.98
Viscosity (cps)	46669 ± 48.31	46621 ± 39.58	46618 ± 34.26	46596 ± 34.11
Spreadability (g.cm/s)	2.74 ± 0.08	2.68 ± 0.06	2.67 ± 0.04	2.59 ± 0.04
Extrudability (%)	85.37 ± 1.64	85.27 ± 1.48	84.91 ± 1.52	84.88 ± 1.36
Drug Content (%)	98.79 ± 1.08	98.64 ± 1.10	98.29 ± 1.05	97.96 ± 1.10
<i>In vitro</i> Released (%)	0 hours	0.24	0.20	0.19
	1 hours	15.3 ± 1.4	15.1 ± 1.2	14.8 ± 1.4
	2 hours	22.6 ± 2.4	21.9 ± 2.4	21.6 ± 2.4
	3 hours	34.7 ± 2.8	33.4 ± 2.6	32.9 ± 2.8
	4 hours	58.2 ± 2.1	57.4 ± 2.2	56.9 ± 2.1
	5 hours	69.1 ± 2.9	68.1 ± 2.7	67.3 ± 2.9
	6 hours	77.5 ± 2.7	76.8 ± 2.4	76.2 ± 2.7
	7 hours	89.2 ± 2.2	88.6 ± 2.1	86.9 ± 2.2
	8 hours	95.1 ± 2.4	94.4 ± 2.6	93.8 ± 2.4

#### 4. CONCLUSION

In current research work, ACV-loaded microemulgels were prepared productively by using a high-pressure homogenizer. Further, the microemulgel was prepared by incorporating ACV microemulsion. The ME formulation showed good results for globule size, zeta potential, and drug entrapment efficiency. Optimize microemulgel showed effective results in appearance, viscosity, pH, spreadability, extrudability, drug content and also *in vitro* diffusion of microemulgel was conducted and showed drug release maximum at 8 hours with a release of more than 95±2.4%, which indicates that ACV is capable of showing better therapeutic efficacy. The transdermal delivery of ACV using microemulgel has been proven to be effective for treating several diseases, and microemulgel shows tremendous potential and will have good clinical implications in the future.

#### Conflict of interest

No conflict of interest.

#### Funding

None to declare.

#### Ethics approval

None to declare.

#### Article info:

Received June 13, 2023

Received in revised form November 17, 2023

Accepted November 18, 2023

#### Author contribution

Conceptualization, BRR. and TST.; methodology, BRR. and TST.; soft-ware, BRR., TST. and AJA.; formal analysis, BRR. and SSP.; investigation, BRR. TST., SSP. and AJA.; re-sources, BRR. and ASJ.; data curation, AJA. and BRR.; writing-original draft preparation, BRR.; AJA. and SSP.; writing-review and editing, BRR. and ASJ.; visualization, BRR. ASJ.; supervision, BRR. All authors have read and agreed to the published version of the manuscript.

#### 5. REFERENCES

- Kondel R, Shafiq N, Kaur IP, Singh MP, Pandey AK, Ratho RK, et al. Effect of acyclovir solid lipid nanoparticles for the treatment of herpes simplex virus (HSV) infection in an animal model of HSV-1 infection. *Pharm Nanotechnol.* 2019;7(5): 389-403.
- Wagstaff AJ, Faulds D, Goa KL. Acyclovir: A reappraisal of its antiviral activity, pharmacokinetic properties and therapeutic efficacy. *Drugs.* 1994;47(1):153-205.
- Bejgum BC, Johnson PR, Stagner WC. Acyclovir chemical kinetics with the discovery and identification of newly reported degradants and degradation pathways involving formaldehyde as a degradant and reactant intermediate. *Int J Pharm.* 2018; 535(1-2):172-9.
- Rastogi V, Yadav P. Transdermal drug delivery system: An overview. *Asian J Pharm.* 2014;6(3):161.

5. Prausnitz MR, Langer R. Transdermal drug delivery. *Nat Biotechnol.* 2008;26(11):1261-8.
6. Murthy SN. Transdermal drug delivery: Approaches and significance. *Res Rep Transdermal Drug Deliv.* 2012;1:1-2.
7. Roohnikan M, Laszlo E, Babity S, Brambilla D. A snapshot of transdermal and topical drug delivery research in Canada. *Pharmaceutics.* 2019;11(6):256.
8. Mohammadi M, Elahimehr Z, Mahboobian MM. Acyclovir-loaded nanoemulsions: Preparation, characterization and irritancy studies for ophthalmic delivery. *Curr Eye Res.* 2021;46(11):1646-52.
9. Ashara KC, Paun JS, Soniwala MM, Chavda JR, Mendapara VP, Mori NM. Microemulgel: An overwhelming approach to improve therapeutic action of drug moiety. *Saudi Pharm J.* 2016;24(4):452-7.
10. Kushwah P, Kumar SP, Koka SS, Gupta A, Sharma R, Darwhekar GN. Microemulgel: A novel approach for topical drug delivery. *J Appl Pharm Res.* 2021;9(3):14-20.
11. Ashara KC, Paun JS, Soniwala MM, Chavada JR, Mori NM. Micro-emulsion based emulgel: A novel topical drug delivery system. *Asian Pac J Trop Dis.* 2014;4:S27-32.
12. Patel BM, Kuchekar AB, Pawar SR. Emulgel approach to formulation development: A review. *Biosci Biotechnol Res Asia.* 2021;18(3):459-65.
13. Nastiti CM, Ponto T, Abd E, Grice JE, Benson HA, Roberts MS. Topical nano and microemulsions for skin delivery. *Pharmaceutics.* 2017;9(4):37.
14. Khullar R, Kumar D, Seth N, Saini S. Formulation and evaluation of mefenamic acid emulgel for topical delivery. *Saudi Pharm J.* 2012;20(1):63-7.
15. Ajazuddin, Alexander A, Khichariya A, Gupta S, Patel RJ, Giri TK, et al. Recent expansions in an emergent novel drug delivery technology: Emulgel. *J Control Release.* 2013;171(2):122-32.
16. Jain N, Jain R, Thakur N, Gupta BP, Jain DK, Banveer J. Nanotechnology: A safe and effective drug delivery system. *Asian J Pharm Clin Res.* 2010;3(3):159-65.
17. Phan HV, Vu TT, Doan CS. Formulation of controlled porosity osmotic pump tablets containing venlafaxine hydrochloride. *Pharm Sci Asia.* 2019;46(2):98-107.
18. Al-Subaie MM, Hosny KM, El-Say KM, Ahmed TA, Aljaeid BM. Utilization of nanotechnology to enhance percutaneous absorption of acyclovir in the treatment of herpes simplex viral infections. *Int J Nanomedicine.* 2015;10:3973-85.
19. Monteiro PF, Silva-Barcellos NM, Caldeira TG, Reis AC, Ribeiro AS, Souza JD. Effects of experimental conditions on solubility measurements for BCS classification in order to improve the biowaiver guidelines. *Braz J Pharm Sci.* 2021;57:e181083.
20. Kashyap A, Das A, Ahmed AB. Formulation and evaluation of transdermal topical gel of ibuprofen. *J Drug Deliv Ther.* 2020;10(2):20-5.
21. Sharma AK, Garg T, Goyal AK, Rath G. Role of microemulsions in advanced drug delivery. *Artif Cells Nanomed Biotechnol.* 2016;44(4):1177-85.
22. Silva AE, Barratt G, Chéron M, Egito ES. Development of oil-in-water microemulsions for the oral delivery of amphotericin B. *Int J Pharm.* 2013;454(2):641-8.
23. Donalisio M, Leone F, Civra A, Spagnolo R, Ozer O, Lembo D, et al. Acyclovir-loaded chitosan nanospheres from nanoemulsion templating for the topical treatment of herpes viruses infections. *Pharmaceutics.* 2018;10(2):46.
24. Moreno MA, Ballesteros MP, Frutos P. Lecithin-based oil-in-water microemulsions for parenteral use: Pseudoternary phase diagrams, characterization and toxicity studies. *J Pharm Sci.* 2003;92(7):1428-37.
25. Mazonde P, Khamanga SM, Walker RB. Design, optimization, manufacture and characterization of efavirenz-loaded flaxseed oil nanoemulsions. *Pharmaceutics.* 2020;12(9):797.
26. Patel S, Jain P, Parkhe G. Formulation and evaluation of acyclovir loaded novel nano-emulsion gel for topical treatment of herpes simplex viral infections. *J Drug Deliv Ther.* 2018;8(5s):265-70.
27. Jiang LC, Basri M, Omar D, Rahman MB, Salleh AB, Rahman RN, et al. Green nano-emulsion intervention for water-soluble glyphosate isopropylamine (IPA) formulations in controlling *Eleusine indica* (*E. indica*). *Pestic Biochem Phys.* 2012;102(1):19-29.
28. Hsieh C, Li P, Lu IC, Wang TH. Preparing glabridin-in-water nanoemulsions by high pressure homogenization with response surface methodology. *J Oleo Sci.* 2012;61(9):483-9.
29. Flourey J, Desrumaux A, Lardières J. Effect of high-pressure homogenization on droplet size distributions and rheological properties of model oil-in-water emulsions. *Innov Food Sci Emerg Technol.* 2000;1(2):127-34.
30. Bhalke RD, Kulkarni SS, Kendre PN, Pande VV, Giri MA. A facile approach to fabrication and characterization of novel herbal microemulsion-based UV shielding cream. *Future J Pharm Sci* 2020;6(1):76.
31. Hasanovic A, Hollick C, Fischinger K, Valenta C. Improvement in physicochemical parameters of DPPC liposomes and increase in skin permeation of acyclovir and minoxidil by the addition of cationic polymers. *Eur J Pharm Biopharm.* 2010;75(2):148-53.
32. Gutiérrez JM, González C, Maestro A, Solè I, Pey CM, Nolla J. Nano-emulsions: New applications and optimization of their preparation. *Curr Opin Colloid Interface.* 2008;13(4):245-51.
33. Sahu P, Kashaw SK, Kushwah V, Sau S, Jain S, Iyer AK. pH responsive biodegradable nanogels for sustained release of bleomycin. *Bioorg Med Chem.* 2017;25(17):4595-613.
34. Restu WK, Sampora Y, Meliana Y, Haryono A. Effect of accelerated stability test on characteristics of emulsion systems with chitosan as a stabilizer. *Procedia Chem.* 2015;16:171-6.
35. Mangalathillam S, Rejinold NS, Nair A, Lakshmanan VK, Nair SV, Jayakumar R. Curcumin loaded chitin nanogels for skin cancer treatment via the transdermal route. *Nanoscale.* 2012;4(1):239-50.
36. Nnamani PO, Ugwu AA, Nnadi OH, Kenechukwu FC, Ofo-kansi KC, Attama AA, et al. Formulation and evaluation of transdermal nanogel for delivery of artemether. *Drug Deliv Transl Res.* 2021;11(4):1655-74.
37. Pathan IB, Dwivedi R, Ambekar W. Formulation and evaluation of ketoprofen loaded chitosan nanogel for pain management: *Ex vivo* and *in vivo* study. *Ars Pharm.* 2019;60(2):101-8.
38. Chaudhary H, Rohilla A, Rathee P, Kumar V. Optimization and formulation design of carbopol loaded piroxicam gel using novel penetration enhancers. *Int J Biol Macromol.* 2013;55:246-53.
39. Gupta DK, Sharma SK, Gaur PK, Singh AP. Lovastatin loaded solid lipid nanoparticles for transdermal delivery: *In vitro* characterization evaluation. *Res J Pharm Technol.* 2022;15(3):1085-9.
40. Maya S, Sarmiento B, Nair A, Rejinold N, Nair S, Jayakumar R. Smart stimuli sensitive nanogels in cancer drug delivery and imaging: A review. *Curr Pharm Des.* 2013;19(41):7203-18.
41. Mishra VK, Bhanja SB, Panigrahi BB. Development and evaluation of nanoemulsion gel for transdermal delivery of valdecoxib. *Res J Pharm Technol.* 2019;12(2):600.
42. Aiyalu R, Govindarjan A, Ramasamy A. Formulation and evaluation of topical herbal gel for the treatment of arthritis in animal model. *Braz J Pharm Sci.* 2016;52(3):493-507.
43. Gandhi A, Jana S, Sen KK. *In vitro* release of acyclovir loaded Eudragit RLPO® nanoparticles for sustained drug delivery. *Int J Biol Macromol.* 2014;67:478-82.
44. Salatin S, Barar J, Barzegar-Jalali M, AdibkiaKh K, Jelvehgari M. Thermosensitive in situ nanocomposite of rivastigmine hydrogen tartrate as an intranasal delivery system: Development, characterization, *ex vivo* permeation and cellular studies. *Colloids Surf B.* 2017;159:629-38.
45. Makwana SB, Patel VA, Parmar SJ. Development and characterization of insitu gel for ophthalmic formulation containing

- ciprofloxacin hydrochloride. *Results Pharma Sci.* 2016;6:1-6.
46. Giri MA, Bhalke RD. Formulation and evaluation of topical anti-inflammatory herbal gel. *Asian J Pharm Clin Res.* 2019; 12(7):252-5.
  47. Dandagi PM, Pandey P, Gadad AP, Mastiholimath VS. Formulation and evaluation of microemulsion based luliconazole gel for topical delivery. *Indian J Pharm Educ Res.* 2020;54(2): 293-301.
  48. Alam MS, Algahtani MS, Ahmad J, Kohli K, Shafiq-un-Nabi S, Warsi MH, et al. Formulation design and evaluation of aceclofenac nanogel for topical application. *Ther Deliv.* 2020;11(12): 767-78.
  49. Kaur R, Ajitha M. Transdermal delivery of fluvastatin loaded nanoemulsion gel: Preparation, characterization and *in vivo* anti-osteoporosis activity. *Eur J Pharm Sci.* 2019;136:104956.
  50. González-González O, Ramirez IO, Ramirez BI, O'Connell P, Ballesteros MP, Torrado JJ, et al. Drug stability: ICH versus accelerated predictive stability studies. *Pharmaceutics.* 2022; 14(11):2324.
  51. Thavva V, Baratam SR. Formulation and evaluation of terbinafine hydrochloride microspoon gel. *Int J Appl Pharm.* 2019; 11(6):78-85
  52. Lordi NG, Scott MW. Stability Charts: Design and application to accelerated stability testing of pharmaceuticals. *J Pharm Sci.* 1965;54(4):531-7.
  53. Charoo NA, Kohli K, Ali A, Anwer A. Ophthalmic delivery of ciprofloxacin hydrochloride from different polymer formulations: *In vitro* and *in vivo* studies. *Drug Dev Ind Pharm.* 2003; 29(2):215-21.
  54. Sharma A, Garg T, Aman A, Panchal K, Sharma R, Kumar S, et al. Nanogel—an advanced drug delivery tool: Current and future. *Artif Cells Nanomed Biotechnol.* 2016;44(1):165-77.
  55. Ali HH, Hussein AA. Oral nanoemulsions of candesartan cilexetil: Formulation, characterization and *In vitro* drug release studies. *AAPS Open.* 2017;3(1):1-6.
  56. Yukuyama MN, Kato ET, de Araujo GL, Löbenberg R, Monteiro LM, Lourenco FR, et al. Olive oil nanoemulsion preparation using high pressure homogenization and d-phase emulsification—a design space approach. *J Drug Deliv Sci Technol.* 2019;49:622-31.
  57. Keerthana K, Sandeep DS. Design, optimization, *in vitro* and *in vivo* evaluation of flurbiprofen loaded solid lipid nanoparticles (SLNs) topical gel. *Indian J Pharm Educ Res.* 2022;56 (4):984-93.
  58. Siddiqui A, Jain P, Thompson SA, Ali A, Hassan N, Haneef J, et al. Investigation of a minocycline-loaded nanoemulgel for the treatment of acne rosacea. *Pharmaceutics.* 2022;14(11): 2322-2.
  59. Azeem A, Rizwan M, Ahmad FJ, Iqbal Z, Khar RK, Aqil M, et al. Nanoemulsion components screening and selection: A technical note. *AAPS PharmSciTech.* 2009;10:69-76.
  60. Hebshy E, Zamora A, Buffa M, Blasco-Moreno A, Trujillo AJ. Characterization of whey protein oil-in-water emulsions with different oil concentrations stabilized by ultra-high pressure homogenization. *Processes.* 2017;5(4):6.
  61. Chaudhari PM, Kuchekar MA. Development and evaluation of nanoemulsion as a carrier for topical delivery system by Box-Behnken design. *Asian J Pharm Clin Res.* 2018;11(8):286-93.
  62. Kadu PJ, Kushare SS, Thacker DD, Gattani SG. Enhancement of oral bioavailability of atorvastatin calcium by self-emulsifying drug delivery systems (SEDDS). *Pharm Dev Technol.* 2011;16(1):65-74.
  63. Lukić M, Pantelić I, Savić SD. Towards optimal pH of the skin and topical formulations: From the current state of the art to tailored products. *Cosmetics.* 2021;8(3):69.
  64. Suvakanta D, Padala NM, Lilakanta N, Prasanta C. Kinetic modeling on drug release from controlled drug delivery systems. *Acta Pol Pharm.* 2010;67(3):217-23.
  65. Fong Yen W, Basri M, Ahmad M, Ismail M. Formulation and evaluation of galantamine gel as drug reservoir in transdermal patch delivery system. *Sci World J.* 2015;2015:495271.